

Journal of Visualized Experiments

High-resolution studies of proteins in natural membranes by solid-state NMR

--Manuscript Draft--

Article Type:	Methods Article - JoVE Produced Video
Manuscript Number:	JoVE62197R2
Full Title:	High-resolution studies of proteins in natural membranes by solid-state NMR
Corresponding Author:	Markus Weingarth Utrecht University: Universiteit Utrecht Utrecht, Utrecht NETHERLANDS
Corresponding Author's Institution:	Utrecht University: Universiteit Utrecht
Corresponding Author E-Mail:	m.g.weingarth@uu.nl
Order of Authors:	Markus Weingarth David Beriashvili Raymond Schellevis Federico Napoli Marc Baldus
Additional Information:	
Question	Response
Please specify the section of the submitted manuscript.	Chemistry
Please indicate whether this article will be Standard Access or Open Access.	Standard Access (US\$2,400)
Please indicate the city, state/province, and country where this article will be filmed . Please do not use abbreviations.	Utrecht, the Netherlands
Please confirm that you have read and agree to the terms and conditions of the author license agreement that applies below:	I agree to the Author License Agreement
Please provide any comments to the journal here.	This is part of the INEXT-Discovery collection (contact: Hans Wienk

TITLE:

High-Resolution Studies of Proteins in Natural Membranes by Solid-State NMR

AUTHORS AND AFFILIATIONS:

David Beriashvili, Raymond D. Schellevis, Federico Napoli, Markus Weingarth, Marc Baldus

NMR Spectroscopy, Bijvoet Centre for Biomolecular Research, Department of Chemistry,
Faculty of Science, Utrecht University, Padualaan 8, 3584 CH, Utrecht, The Netherlands

Correspondence to:

Markus Weingarth (m.weingarth@uu.nl)

Marc Baldus (m.baldus@uu.nl)

Email Addresses of Co-Authors:

David Beriashvili (d.beriashvili@uu.nl)

Raymond Schellevis (r.d.schellevis@uu.nl)

Federico Napoli (f.napoli@students.uu.nl)

Markus Weingarth (m.weingarth@uu.nl)

Marc Baldus (m.baldus@uu.nl)

KEYWORDS:

solid-state NMR, membrane proteins, structural biology, dynamic nuclear polarization, BamA, KcsA

SUMMARY:

This work details robust basic routines on how to prepare isotope-labeled membrane protein samples and analyze them at high-resolution with modern solid-state NMR spectroscopy methods.

ABSTRACT:

Membrane proteins are vital for cell function and thus represent important drug targets. Solid-state Nuclear Magnetic Resonance (ssNMR) spectroscopy offers a unique access to probe the structure and dynamics of such proteins in biological membranes of increasing complexity. Here, we present modern solid-state NMR spectroscopy as a tool to study structure and dynamics of proteins in natural lipid membranes and at atomic scale. Such spectroscopic studies profit from the use of high-sensitivity ssNMR methods, i.e., proton-(¹H)-detected ssNMR and DNP (Dynamic Nuclear Polarization) supported ssNMR. Using bacterial outer membrane beta-barrel protein BamA and the ion channel KcsA, we present methods to prepare isotope-labeled membrane proteins and to derive structural and motional information by ssNMR.

INTRODUCTION:

Structural and motional studies of membrane proteins in physiologically relevant environments pose a challenge to traditional structural biology techniques¹. Modern solid-state nuclear magnetic resonance spectroscopy (ssNMR) methods offer a unique approach for the

characterization of membrane proteins²⁻⁷ and has long been used to study membrane proteins, including membrane embedded protein pumps⁸, channels⁹⁻¹¹, or receptors¹²⁻¹⁵. Technical advances such as ultra-high magnetic fields >1,000 MHz, fast magic angle spinning frequencies >100 kHz, and hyperpolarization techniques¹⁶ have established ssNMR as a powerful method for the study of membrane proteins in environments of ever-increasing complexity from liposomes to cell membranes and even whole cells. For example, DNP has become a powerful tool for such experiments (see reference¹⁷⁻²⁵). More recently, ¹H-detected ssNMR offers increasing possibilities to study membrane proteins at high spectral resolution and sensitivity^{25-28,29}. This work highlights two bacterial membrane proteins that are involved in essential functions, i.e., protein insertion and ion transport. The corresponding proteins, BamA^{25,30-33} and KcsA^{23,27,28,34-39} (or chimeric variants thereof^{10,40}) have been examined by ssNMR methods for more than a decade.

A representative protocol for the preparation and ssNMR characterization of bacterially originating membrane proteins is presented here. The different steps of the protocol are shown in **Figure 1**. First, the expression, isotope-labeling, purification, and membrane-reconstitution of BamA is explained. Then, a general workflow for the characterization of the membrane protein by ssNMR is presented; specifically, the assignment of membrane protein backbones using ¹H-detected ssNMR at fast magic angle spinning. Finally, basic setup and acquisition of dynamic nuclear polarization-(DNP)-supported experiments, which significantly boost ssNMR signal sensitivity, are detailed.

PROTOCOL:

1. Production of uniformly labeled ²H,¹³C,¹⁵N-labeled BamA-P4P5

NOTE: While this protocol requires working with non-pathogenic Gram-negative bacteria, adherence to basic biological safety procedures is a must, namely, wearing safety glasses, lab coats, gloves, and following institutional standard operating procedures for work with microorganisms.

1.1. Use a single colony of *E. coli* BL 21 Star (DE3) containing the pET11aAssYaeT plasmid encoding for *E. coli* BamA-P4P5 to inoculate 50 mL of Lysogeny broth supplemented with 50 µg/L of ampicillin.

1.2. Grow the culture at 37 °C at 200 rpm until an OD₆₀₀ of 0.6 is reached. Spin at 2,000 x g for 10 min. Resuspend the pellet in 50 mL of M9 (see **Table 1**) to a maximum OD₆₀₀ of 0.1.

NOTE: All future growing steps take place at the conditions stated above unless otherwise noted.

1.3. Grow the culture until OD₆₀₀ of 0.5. Spin at 2,000 x g for 10 min at room temperature. Resuspend the pellet in 50 mL of M9 containing 90% D₂O (see **Table 1** for recipe) to a maximum OD₆₀₀ of 0.1. Grow the culture overnight at 30 °C at 200 rpm.

1.4. Spin down the culture at 2,000 x *g* for 10 min at room temperature. Resuspend the pellet in the prewarmed 50 mL 90% D₂O M9 to a maximum OD₆₀₀ of 0.1. Grow until an OD₆₀₀ of 1.0 is reached.

1.5. Spin down the culture at 2,000 x *g* for 10 min at room temperature. Prepare 100 mL of 100% D₂O M9 medium with isotope-enriched amounts of non-enriched glucose and ammonium chloride. Resuspend in 100% D₂O M9 medium to a maximum OD₆₀₀ of 0.1. Grow until an OD₆₀₀ of 0.7 is reached.

1.6. Spin down the culture at 2,000 x *g* for 10 min at room temperature. Discard the supernatant and resuspend the pellet in 500 mL of 100% D₂O M9 medium with isotopes (see **Table 1**) to a maximum OD₆₀₀ of 0.1.

1.7. Allow the culture to grow until an OD₆₀₀ of 0.6–0.9 is reached. Induce with 1 mM of isopropyl β-D-1-thiogalactopyranoside (IPTG). Express for 4 h and harvest cells at 4,000 x *g* for 15 min at room temperature.

1.8. Purification, refolding, and BamA-P4P5 proteo-liposome formation

NOTE: All the steps of this section should be conducted in a fume hood. Special care must be taken when opening tubes post-centrifugation—limits harmful aerosols.

1.8.1. Thaw the pellet on ice. Resuspend the pellet in 20 mL of cold Buffer 1. See **Table 2** for the Buffers.

1.8.2. Spin down the solution at 4,000 x *g* for 20 min at 4 °C. Resuspend the pellet in 20 mL of cold distilled H₂O. Allow the suspension to incubate on ice for 10 min.

1.8.3. Spin down the suspension at 4,000 x *g* for 20 min at 4 °C. Resuspend in 10 mL cold Buffer 2 and allow to incubate on ice for 30 min.

1.8.4. Supplement the mixture with an additional 10 mL of cold buffer 2 and incubate for a further 30 min on ice. Add 0.5% n-Dodecyl-B-D-Maltoside (DDM) and swirl gently.

1.8.5. Sonicate the sample on ice at 13 kHz until viscous—use 10 s long on/off pulses. Spin down at 25,000 x *g* for 20 min at 4 °C. Wash three times with 20 mL of Buffer 3. Centrifuge at 25,000 x *g* for 20 min at 4 °C.

1.8.6. Resuspend the pellet in 20 mL of Buffer 4. Incubate at 37 °C for 30 min. Sonicate the sample on ice at 13 kHz, until clear—use 10 s long on/off pulses.

1.8.7. Spin down the sample at 25,000 x *g* for 20 min at 4 °C. Repeat steps 1.8.4 to 1.8.6 omitting addition of protease inhibitor and incubation at 37 °C.

1.8.8. Wash the pellet with 20 mL of water and twice with Buffer 3. Spin down at 25,000 x *g* for 20 min at 4 °C. Aliquot the suspension into 1 mL microcentrifuge tubes and spin the microcentrifuge tubes at maximum speed on a bench-top centrifuge for 20 min. Inclusion body purity is assessed by 10% SDS-Page gel, see **Figure 2A**. Expected yield for purified BamA-P4P5 triply (²H,¹³C,¹⁵N) labeled is 30 mg/L.

1.8.9. Solubilize inclusion bodies in 200 µL of Buffer 5 and 300 µL of H₂O. Add 6M guanidium chloride (GdnCl). Adjust the volume of microcentrifuge tube to 1 mL with H₂O. Vortex the mixture and incubate for 4 h at room temperature. Vortex the microcentrifuge tubes periodically (every 30 min).

1.8.10. Spin at 100,000 x *g* for 1 h at 4 °C. Use Beer-Lambert's Law to determine protein concentration by 280 nm. The molar extinction coefficient is 117,120 M⁻¹cm⁻¹. If concentration is >100 µM dilute with 1x Buffer 5 with 6 M GdnCl. Rapidly dilute the protein 10x in Buffer 6. Incubate the mixture overnight at room temperature.

NOTE: For ultracentrifugation, use ultracentrifugation grade 1.5 mL tubes.

1.8.11. Determine refolding efficiency using a semi-native SDS-Page gel. Take two 10 µL aliquots from step 1.8.10 and add 10 µL of Laemmli buffer (buffer 8) to each aliquot. Boil one sample for 10 min at 95 °C; leave the other aliquot on ice. Afterwards, run both samples at 14 mA on a 10% SDS-Page gel. The stacking and running portions of the gels lack reducing agent and SDS. Protein staining is achieved using Coomassie dye. The expected results are shown in **Figure 2B**.

1.8.12. Spin down the sample at 4,000 x *g* for 20 min at 4 °C. Concentrate the sample to a working volume of 8 mL using a 30 kDa centrifugal filter. Spin the sample at 4,000 x *g* for 20 min at 4 °C. Measure protein absorbance at 280 nm. As in step 1.8.10, determine the protein concentration.

1.8.13. Calculate the amount of lipid required for a 10:1 lipid to protein ratio (LPR–mol/mol). From a chloroform stock, add the required amount of lipids, as calculated in step 1.8.12, into a 100 mL round bottom flask (RBF). Evacuate the chloroform from the RBF under a gentle stream of nitrogen. Place RBF on high vacuum for 3 h. Hydrate the lipid film with 1 mL of Buffer 7. Incubate RBF for 10 min at 37 °C.

1.8.14. Add the protein mixture (from step 1.8.12) to the RBF.

1.8.15. Dilute the protein/lipid mixture (from step 1.8.14) to the final volume of 50 mL in the RBF. Use Buffer 7 supplemented with 1x protease inhibitor dissolved in DMSO and incubate for 30 min at 37 °C.

1.8.16. Dialyze against 100 volumes of Buffer 7 for 2 weeks (use 12–14 kDa molecular weight cut-off dialysis tubing). For the first 24 h, perform the dialysis at room temperature with addition of fresh Buffer 7 every 8 h. Afterwards, change the buffer once daily, and perform dialysis at 4 °C.

2. Filling of the ssNMR rotor

2.1. After step 1.8.16, centrifuge for 30–60 min at 10,000 x *g* at 4 °C so that a pellet is formed. Remove the supernatant with a pipette.

NOTE: The technique discussed below has been optimized for a 3.2 mm rotor but is applicable for almost any rotor diameter.

2.2. Pipette the sample into the rotor and gently spin the same down with a table centrifuge.

NOTE: Depending on sample consistency, one may either use a densification tool to compact the sample, or a spatula instead of a pipette to put the sample into the rotor.

2.3. Repeat this process 2-3x until the rotor is filled to the correct height and check if there is enough space for the cap left, as indicated by the marker line on the densification tool. Close the rotor with the cap positioning tool on an even surface. Mark half the bottom edge of the rotor.

NOTE: New ssNMR rotor generations come with a durable laser mark at the bottom edge for the optical detection of the rotor spinning frequency. Otherwise, the use of a sharpie pen is suggested; as the MAS detector has been optimized specifically for sharpie ink.

2.4. Use a magnifying glass to check whether the cap is well placed.

3. Sample characterization by 2D ¹³C-¹³C ssNMR spectroscopy

3.1. Insert the rotor into the magnet, using the automatic spinning routine of the MAS unit, spin the sample up to the desired MAS frequency between 10 and 20 kHz MAS while cooling the sample to 270 K set temperature. Tune and match the ¹H and ¹³C channels.

NOTE: For the choice of the MAS frequency, avoid accidentally matching the chemical shift distance between the spectral C α region and the Carbonyl carbon region to the spinning frequency, i.e., avoid the first order rotational resonance condition⁴¹.

3.2. Optimize a ¹H-¹³C cross-polarization⁴² (CP) experiment by varying the rf power on the proton channel from 25-80 kHz. Typical parameters are 45 kHz rf power on ¹³C, 80–100 kHz heteronuclear ¹H-decoupling⁴³ during acquisition, 1.8–2.0 s recycle delay, and 64 scans.

3.2.1. Optimize the CP contact time for maximal signal sensitivity on the aliphatic carbons.

3.2.2. Determine ¹H 90° pulse length in the ¹³C-CP experiment by multiplying the starting pulse by four, i.e., by optimizing a 360° pulse, and vary the length until the signal has disappeared. Include a rectangular pulse directly after the CP transfer and optimize the ¹³C 90° pulse length analogously.

3.3. Run a 2D ^{13}C - ^{13}C proton-driven spin diffusion (PDSF)-type experiment such as PARIS with 30 ms magnetization transfer time to detect intra-residual correlations and gauge the sample quality. Transfer the power-levels, the contact time, and 90° pulse lengths from the previously optimized ^{13}C -CP experiment. Use an acquisition time of 4–6 ms in the indirect dimension. Process the spectrum with squared sin bell functions (QSIN) or, for insensitive samples, exponential line broadening in both dimensions.

3.4. Extract slices of isolated cross-peaks and determine the linewidth at half heights. A linewidth between ~ 0.3 – 1.0 ^{13}C ppm is indicative of a well-ordered sample, ideal for ssNMR characterization, whereas a linewidth above 1.0 ^{13}C ppm is indicative of conformational heterogeneity that may compromise ssNMR characterization. The 2D CC PARIS spectrum of BamA shown in **Figure 3A** is an example of a well-ordered protein that gives high-quality spectra.

4. Backbone assignment by ^1H -detected 3D ssNMR spectroscopy

4.1. Acquisition of 2D NH spectral fingerprints

4.1.1. Fill the sample in a 1.3 mm rotor, as described above. Insert the rotor into the magnet, spin the sample to 10–20 kHz MAS and cool the sample to 240–250 K set temperature or lower, depending on the specifications of the ssNMR probehead. Use the MAS unit interface to increase the MAS frequency gradually in steps of 5 kHz to 60 kHz MAS.

4.1.2. Optimize the CP amplitudes, contact times, and 90° pulse lengths in ^{13}C - and ^{15}N CP experiments. Use amplitudes around 30–50 or 70–100 kHz on the heteronuclear channels and vary the amplitude on the ^1H -channel from 80–180 kHz. Use a recycling delay of 0.7–1.2 s, along with 15 kHz low-power heteronuclear proton decoupling⁴⁴. Also, see reference⁴⁵ for further practical details on how to set up CP ssNMR experiments.

4.1.3. Acquire a 2D NH experiment to gauge the ^1H -resolution. Transfer the ^{15}N -CP parameters and use approximately 15 and 25 ms acquisition time in the direct and indirect dimensions. For the first ^1H to ^{15}N CP transfer, use the previously optimized contact time. For the ^{15}N to ^1H backtransfer, use 0.7–1.0 ms contact time to minimize interresidual magnetization transfer.

4.1.4. Use 50–250 ms water MISSISSIPPI suppression⁴⁶, dependent on sample water content. Process the spectrum with squared sin bell functions (QSIN) in both dimensions. Extract slices of isolated cross-peaks and determine the linewidth at half heights. An example for a high-quality 2D NH spectrum²⁵ is shown for membrane-embedded BamA-P4P5 in **Figure 3B**.

4.2. Backbone assignments

4.2.1. Optimize a 1D ^{15}N to ^{13}C specific CP experiment⁴⁷. Place the ^{13}C carrier in the middle of the $\text{C}\alpha$ region around 55 ppm. Use a ^{13}C rf amplitude of 20 kHz and vary the ^{15}N amplitude from 35 to 45 kHz for maximal transfer to the $\text{C}\alpha$ signals and minimal transfer to the carbonyl signals. Optimize the contact time from 3 to 10 ms in increments of 1 ms.

4.2.2. Run a 3D CαNH experiment. Transfer all CP amplitudes, contact times, and pulse lengths from the previously optimized steps. Use approximately 10 ms and 30 ms in the indirect and direct acquisition dimensions. Process the spectrum with squared sin bell functions (QSIN) in all three dimensions.

4.2.3. Optimize a 1D Cα to CO DREAM magnetization transfer⁴⁸. Start with a ¹⁵N to ¹³Cα specific CP transfer. Then, transfer the magnetization from Cα to CO using a spin lock on the ¹³C channel. Vary the *rf* amplitude from 20 to 35 kHz for optimal transfer. Optimize the transfer time from 4 to 10 ms.

4.2.4. Run a 3D Cα(CO)NH experiment. Transfer all *rf* amplitudes, contact times, and pulse lengths from the previously optimized steps. Use approximately 10 ms and 30 ms in the indirect and direct acquisition dimensions. Process the spectrum with squared sin bell functions (QSIN) in all three dimensions.

4.2.5. Repeat and adapt steps 1–4 for the analogous 3D CONH and CO(Cα)NH experiments. Use this quartet of 3D experiments for sequential Cα and CO walks to assign the protein backbone, as shown on the example of KcsA in **Figure 4**²⁸.

5. Protein dynamics by ¹H-detected ssNMR spectroscopy

5.1. For ¹⁵N T₁ studies, use the previously optimized 2D NH experiment at 60 kHz MAS and include a delay after the first ¹H to ¹⁵N cross-polarization step. Acquire a series of 2D NH experiments and vary the delay from 0 to 16 s using steps of, e.g., 0, 2, 4, 8, and 16 s.

5.2. Plot the normalized intensities for resolved signals as a function of the increasing delay time. Fit the T₁ decay to single exponentials according to $y = \exp(-x/T_1)$, with *y* being the signal intensity at decay time *x*.

5.3. Analogously, for ¹⁵N T_{1rho} studies, include a spin-lock pulse in the pulse program on the ¹⁵N channel with an *rf* amplitude between 15–20 kHz after the first ¹H to ¹⁵N cross-polarization step^{26,49}. Acquire a series of 2D NH experiments and vary the delay from 0 to 150 ms and fit the T_{1rho} decay of resolved signals to single exponentials. Illustrative ¹⁵N T_{1rho} data is shown for membrane-embedded K⁺ channels in **Figure 5**^{27,28}.

6. Dynamic nuclear polarization

NOTE: The following preparative steps relate to the use of a commercial DNP setups using 3.2 mm sapphire MAS rotors (**Figure 6**)²⁰. Use of the zirconia rotors or other DNP equipment may lead to lower DNP signal enhancements.

6.1. Resuspend membrane protein pellet (from step 2.1) in 50 μL of deuterated DNP buffer (60% (v/v) deuterated d₈- and glycerol, and 15 mM AMUPol⁵⁰. For experiments at 800 MHz, we

recommend using 10 mM NATriPOL-3⁵¹. Also see reference⁵² for further practical aspects to DNP ssNMR experiments.

6.2. Centrifuge for 10–20 min at 100,000 x *g* at 4 °C so that a pellet is formed. Remove the supernatant with a pipette.

6.3. Precool the centrifugal adaptor and the 3.2 mm sapphire MAS rotor components to <4 °C. The following steps (6.4–6.7) need to be done as quickly as possible to prevent the DNP agents from getting reduced.

6.4. Place the 3.2 mm sapphire rotor in the centrifuge adapter and fill it with the suspension of proteo-liposomes from step 6.2.

6.5. Pipette the resuspended membrane protein sample against the inner wall of the rotor carefully using a 200 µL pipette tip. Allow the solution to slide down to the bottom of the rotor. Ensure that air bubbles are not formed.

6.6. Spin down the sample in the rotor for 5–10 mins at 4,500 x *g* at 4 °C. Remove the supernatant containing excess DNP juice by pipetting it out carefully without disrupting the cell pellet. Repeat steps 6.4–6.6 until the rotor is full.

6.7. Carefully position the polytetrafluoroethylene (PTFE) spacer using the spacer screw on top of the rotor.

6.8. Place the rotor, cap side down in a rotor plunger⁵³ and plunge the rotor into liquid nitrogen. Allow at least 30–60 s for the rotor and the sample to freeze.

6.9. Start up the heat exchanger unit and cool down the DNP probe to ~90K.

6.10. Set the MAS unit to **Manual mode** and set the variable temperature (VT) to 135 l/h and bearing and drive gas flows to ~6 l/h.

6.11. Engage **Eject** on the MAS console.

6.12. Transfer the frozen sample from Step 6.8 from the liquid N2 into the sample catcher and place it in the probe (also see reference⁵³).

6.13. Manually increase the probe bearing pressure (Bp) to ~500 mbar before engaging the “Insert”. This is advisable for stable and safe spinning of the rotor.

6.14. Increase MAS rate to the desired value using the procedure described in reference⁵³.

6.15. Check for DNP enhancements with and without microwaves using a standard 1D CP experiments (also see, e.g., reference^{51,54}) (**Figure 7**) before proceeding with multidimensional

experiments, e.g., 2D CC experiments described in section 3 of this article.

REPRESENTATIVE RESULTS:

Figure 2 shows representative gels for inclusion body purity (Panel A) and refolding of inclusion bodies (Panel B3). **Figure 2** confirms the successful purification of ^{13}C , ^{15}N -labeled BamA-P4P5.

Figure 3A shows a typical 2D ^{13}C - ^{13}C spectrum of a well-ordered membrane protein, and **Figure 3B** shows a typical, high-quality 2D ^{15}N - ^1H spectrum of a perdeuterated membrane protein²⁵. Note that this membrane protein expressed as inclusion bodies, so that the transmembrane part is also accessible by perdeuteration. For membrane proteins that do not express in inclusion bodies, one usually needs to employ H_2O -based growth media^{27,55–57}.

Figure 4 exemplifies how to assign the backbone of membrane proteins using ^1H -detected 3D experiments²⁸. **Figure 5** demonstrates the power of ssNMR relaxation measurements that can provide detailed, site-resolved information on the dynamics of membrane proteins^{28,49}.

Eventually, **Figure 6** and **Figure 7** illustrate how DNP can boost the sensitivity of ssNMR experiments of membrane-embedded proteins²⁵. **Figure 6** shows high-resolution DNP-supported ssNMR information on the structure of the outer-membrane protein BamA.

FIGURE AND TABLE LEGENDS:

Figure 1: Experimental methodology for atomic-level multidimensional solid-state nuclear magnetic resonance (ssNMR) studies of membrane proteins embedded in native-membrane environments. Specifically, the workflow details robust procedures for membrane protein production, purification, refolding, proteo-liposomes formation, and most crucially setup/acquisition/analysis of cutting-edge multidimensional ssNMR spectra.

Figure 2: Representative gels for inclusion body purity and refolding. (A) 10% SDS-Page gel of BamA-P4P5 inclusion bodies. Lane A has the molecular weight ladder; Lane B has BamA-P4P5 inclusion bodies. The expected molecular weight of BamA-P4P5 is 61.1 kDa. (B) 10% SDS-page semi native gel for assessing BamA-P4P5 refolding efficiency. Lane A contains the boiled sample; as expected, it migrates to the molecular weight of 61.1 kDa. Lane B contains the un-boiled sample; the top band is protein that has remained unfolded and the bottom band near 37 kDa is the folded population. The folding efficiency can be determined using image analysis software—in this specific case, folding efficiency is >70%.

Figure 3: Representative 2D ^{13}C - ^{13}C PARIS and ^1H -detected NH spectra for BamA-P4P5 proteo-liposomes. (A) 2D ^{13}C - ^{13}C PARIS spectrum of ^{13}C , ^{15}N -labeled BamA-P4P5 in liposomes. The spectrum was acquired at 700 MHz (^1H -frequency) magnetic field using 13 kHz MAS and a ^{13}C - ^{13}C magnetization transfer time of 30 ms. (B) ^1H -detected 2D NH spectrum of the ^2H , ^{13}C , ^{15}N -labeled transmembrane part of BamA in liposomes. The spectrum was acquired at 800 MHz (^1H -frequency) and 60 kHz MAS. This figure has been modified from reference²⁵.

Figure 4: Sequential ssNMR assignments of membrane-embedded ion channels with ^1H -detected 3D experiments. Upper panel: $\text{C}\alpha$ - $\text{C}\alpha+1$ backbone walk showing full connectivity for residues T72–Y82 in KcsA mutant E71A. Dark blue signals show $\text{C}\alpha\text{H}$ planes from a 3D $\text{C}\alpha\text{NH}$ experiment, cyan $\text{C}\alpha\text{H}$ planes were taken from a 3D $\text{C}\alpha\text{coNH}$ experiment. Lower panel: CO-1-CO backbone walk showing full connectivity for residues T72–Y82 in E71A. Magenta signals show COH planes from a 3D CONH experiment, red COH planes were taken from a 3D COc^2NH experiment. This figure has been modified from reference²⁸.

Figure 5: SSNMR ^{15}N $T_{1\rho}$ data reveal differential dynamics in membrane-embedded point-mutants of the bacterial potassium channel KcsA. (A) ^{15}N rotating frame ssNMR relaxation rates ($R_{1\rho}$) that report on slow molecular motions in WT KcsA (cyan), E71A (red), E71I (blue), and E71Q (orange) measured at 700 MHz and 58 kHz MAS. The error bars show the standard error of the fit. (B) Illustration of the site-resolved selectivity filter dynamics. The size of the magenta spheres represents the $R_{1\rho}$ relaxation rates. This figure has been modified from reference²⁸.

Figure 6: Preparation of proteo-liposomes for dynamic nuclear polarization (DNP) NMR experiments. Important steps are highlighted, including resuspension of proteo-liposomes in DNP juice, packing the sample into a sapphire rotor, and ultimately execution of DNP measurements.

Figure 7: DNP spectra of ^{13}C and ^{15}N -labeled BamA-P4P5. Left: A DNP signal enhancement of about 110 could be obtained for membrane-embedded ^{13}C , ^{15}N -IFG-labeled BamAP4P5 using a 400 MHz/263 GHz DNP system. Right: Close-up of the $\text{C}\alpha$ - $\text{C}\beta$ region of the DNP enhanced ^{15}N -edited carbon-carbon correlation experiment⁵⁸ using a long (1 s) mixing time, measured on ^{13}C , ^{15}N -IFG-labeled BamAP4P5, in the presence (red spectrum) and absence (blue spectrum) of unlabeled BamCDE. Crosses are the tentative assignments for the residues targeted by these experiments. Schematic representation of the correlations observed between β -strand 1 and 16 in ^{15}N -edited $\text{C}_\alpha\text{C}_\alpha$ DNP spectra for the case of a lateral gate open. The distance between $\text{C}\alpha$ residues of the closest residue in $\beta 1$ to the I806 of $\beta 16$ is indicated. This figure has been modified from reference²⁵.

Table 1: M9 minimal medium recipe. The medium can be made up in H_2O or varying amounts of D_2O as directed by the protocol. *In case of perdeuterated protein production D-Glucose- $^{13}\text{C}_6,1,2,3,4,5,6,6\text{-d}_7$ is used.

Table 2: Buffers used for the sample preparation of membrane embedded BamA.

Table 3: Micronutrients stock (1,000x). The stock can be made up in water or varying amounts of D_2O as directed by the protocol.

Table 4: Vitamin Supplement (1,000x) for 100 mL. The supplement can be made up in H_2O or varying amounts of D_2O as directed by the protocol.

DISCUSSION:

Membrane proteins are key players in the regulation of vital cellular functions both in prokaryotic and eukaryotic organisms; thus, understanding their action mechanisms at atomic levels of resolution is of vital importance. The existing structural biology techniques have pushed scientific understanding of membrane proteins quite far but have heavily relied on experimental data gathered from in vitro systems devoid of membranes. In this article, an experimental approach is presented that allows to obtain atomistic insight into the structure and function of two bacterial membrane-proteins embedded in native-like membrane by utilizing cutting-edge solid-state NMR techniques, namely, fast-MAS and DNP. This method is broadly applicable to other bacterial membrane proteins.

The protocol begins by describing a robust methodology to produce and purify triply isotope labeled BamA in high yield and purity (**Figure 2A**)—other stable-isotope labeling schemes can be employed. The purification protocol makes use of synergy between surfactant activity and sonication to remove cellular debris from BamA inclusion bodies. The subsequent refolding sees formation of BamA-LDAO micelles (**Figure 2B**). Further addition of lipids and dialysis aids in the removal of LDAO and residual surfactant molecules thereby facilitating formation of proteo-liposomes suitable for solid-state NMR studies. The formation of proteo-liposomes is a crucial step and must be done with adherence to the buffer exchange schedule detailed above. This is mandatory for a successful preparation.

The acquisition of 2D spin diffusion-based CC spectra (**Figure 3A**) of membrane proteins is routine and often among the first experiments conducted to gauge the sample's quality and secondary structure content. By using long CC mixing times, these experiments can also be conveniently used to derive structural information. Note that spin diffusion transfer efficacy inversely scales with the MAS frequency. Hence, longer mixing times are required with increasing MAS frequency.

If the membrane-protein is grown in D₂O-based buffers as in the representative example of **Figure 3B**, it is necessary to back-exchange the amino-protons in H₂O-based buffers afterwards⁵⁹. This may prevent the detection of the water-inaccessible transmembrane-part. This limitation can be overcome by the use of dedicated H₂O-based growth media²⁷ or fully-protonated membrane proteins in combination with MAS frequencies above 100 kHz^{55–57,60}.

Spectral assignments of small membrane proteins can be conveniently performed with the quartet of ¹H-detected 3D experiments that is shown in **Figure 4** for the selective filter of the K⁺ channel E71A KcsA²⁸. This quartet can be supplemented by a 3D CαCαNH experiment or 2D CC experiments to obtain sidechain information that simplifies the assignments. For larger membrane proteins, the use of 4D or higher order experiments is necessary to disambiguate the assignments. These spectra are usually acquired with dedicated non-uniform sampling strategies in order to shorten experimental time.

Detailed relaxation data is shown in **Figure 5** for the K⁺ channel KcsA and three KcsA point mutants with different gating behaviors, hence correlation membrane protein dynamics to function²⁸. For example, compared to the WT KcsA channel, the constitutively active mutant E71A shows a striking rigidification, and the so-called “flicker” mutant E71Q shows a marked

increase in global protein dynamics. For relaxation measurements, a high sensitivity is indispensable because signals toward the end of the relaxation series also need to be acquired with robust signal-to-noise ratios.

The spectacular advantages of DNP are shown in **Figure 6** and **Figure 7**. DNP can strongly improve sensitivity in ssNMR experiments that enable otherwise infeasible experiments^{27,61–63}. In **Figure 7B**, we utilized DNP to probe residue-specific, through-space contacts in a membrane-embedded BamA (547 residues)-Bam CDE complex. A combination of amino-acid specific labeling and DNP-supported ¹⁵N-edited ¹³C-¹³C correlation spectroscopy⁵⁸ allows to probe through-space contacts between α -strands 1 and 16, suggesting the so-called lateral gate that is critical for function (see, e.g., reference⁶⁴) is open.

In the future, we expect modern solid-state NMR methods to continue to play a major role for structural and dynamical studies of membrane proteins, especially in complex media such as cellular preparations and whole cells.

ACKNOWLEDGMENTS:

This work is part of the research programs ECHO, TOP, TOP-PUNT, VICI, and VIDI with project numbers 723.014.003, 711.018.001, 700.26.121, 700.10.443, and 718.015.00, which are financed by the Dutch Research Council (NWO).

DISCLOSURES:

The authors have nothing to disclose.

REFERENCES:

1. Weingarth, M., Baldus, M. Solid-state NMR-based approaches for supramolecular structure elucidation. *Accounts of Chemical Research*. **46** (9), 2037–2046 (2013).
2. Kaplan, M., Pinto, C., Houben, K., Baldus, M. Nuclear magnetic resonance (NMR) applied to membrane-protein complexes. *Quarterly Reviews of Biophysics*. **49**, e15 (2016).
3. Brown, L. S., Ladizhansky, V. Membrane proteins in their native habitat as seen by solid-state NMR spectroscopy. *Protein Science*. **24** (9), 1333–1346 (2015).
4. Ladizhansky, V. Applications of solid-state NMR to membrane proteins. *Biochimica Et Biophysica Acta. Proteins and Proteomics*. **1865** (11 Pt B), 1577–1586 (2017).
5. Hong, M., Zhang, Y., Hu, F. H. Membrane protein structure and dynamics from NMR spectroscopy. *Annual Review of Physical Chemistry*. **63**, 1–24 (2012).
6. Shahid, S. A. et al. Membrane-protein structure determination by solid-state NMR spectroscopy of microcrystals. *Nature Methods*. **9** (12), 1212–1217 (2012).
7. Wang, S. L. et al. Solid-state NMR spectroscopy structure determination of a lipid-embedded heptahelical membrane protein. *Nature Methods*. **10** (10), 1007–1012 (2013).
8. Herzfeld, J., Lansing, J. C. Magnetic resonance studies of the bacteriorhodopsin pump cycle. *Annual Review of Biophysics and Biomolecular Structure*. **31** (1), 73–95 (2002).
9. Ketchum, R. R., Hu, W., Cross, T. A. High-resolution conformation of gramicidin A in a lipid bilayer by solid-state NMR. *Science*. **261** (5127), 1457–1460 (1993).

- 529 10. Lange, A. et al. Toxin-induced conformational changes in a potassium channel revealed
530 by solid-state NMR. *Nature*. **440** (7086), 959–962 (2006).
- 531 11. Cady, S. D. et al. Structure of the amantadine binding site of influenza M2 proton channels
532 in lipid bilayers. *Nature*. **463** (7281), 689–692 (2010).
- 533 12. Park, S. H. et al. Structure of the chemokine receptor CXCR1 in phospholipid bilayers.
534 *Nature*. **491** (7426), 779–783 (2012).
- 535 13. Luca, S. et al. The conformation of neurotensin bound to its G protein-coupled receptor.
536 *Proceedings of the National Academy of Sciences of the United States of America*. **100** (19),
537 10706–10711 (2003).
- 538 14. Joedicke, L. et al. The molecular basis of subtype selectivity of human kinin G-protein-
539 coupled receptors. *Nature Chemical Biology*. **14** (3), 284–290 (2018).
- 540 15. Krug, U. et al. The conformational equilibrium of the neuropeptide Y2 receptor in bilayer
541 membranes. *Angewandte Chemie (International Edition in English)*. **59** (52), 23854–23861 (2020).
- 542 16. Maly, T. et al. Dynamic nuclear polarization at high magnetic fields. *Journal of Chemical*
543 *Physics*. **128** (5) (2008).
- 544 17. Bajaj, V. S., Mak-Jurkauskas, M. L., Belenky, M., Herzfeld, J., Griffin, R. G. Functional and
545 shunt states of bacteriorhodopsin resolved by 250 GHz dynamic nuclear polarization–enhanced
546 solid-state NMR. *Proceedings of the National Academy of Sciences of the United States of*
547 *America*. **106** (23), 9244–9249 (2009).
- 548 18. Linden, A. H. et al. Neurotoxin II bound to acetylcholine receptors in native membranes
549 studied by dynamic nuclear polarization NMR. *Journal of the American Chemical Society*. **133** (48),
550 19266–19269 (2011).
- 551 19. Ong, Y. S., Lakatos, A., Becker-Baldus, J., Pos, K. M., Glaubitz, C. Detecting substrates
552 bound to the secondary multidrug efflux pump EmrE by DNP-enhanced solid-state NMR. *Journal*
553 *of the American Chemical Society*. **135** (42), 15754–15762 (2013).
- 554 20. Koers, E. J. et al. NMR-based structural biology enhanced by dynamic nuclear polarization
555 at high magnetic field. *Journal of Biomolecular NMR*. **60** (2–3), 157–168 (2014).
- 556 21. Becker-Baldus, J. et al. Enlightening the photoactive site of channelrhodopsin-2 by DNP-
557 enhanced solid-state NMR spectroscopy. *Proceedings of the National Academy of Sciences of the*
558 *United States of America*. **112** (32), 9896–9901 (2015).
- 559 22. Kaplan, M. et al. EGFR dynamics change during activation in native membranes as
560 revealed by NMR. *Cell*. **167** (5), 1241–1251 (2016).
- 561 23. Visscher, K. M. et al. Supramolecular organization and functional implications of K⁺
562 channel clusters in membranes. *Angewandte Chemie (International Edition in English)*. **56** (43),
563 13222–13227 (2017).
- 564 24. Joedicke, L. et al. The molecular basis of subtype selectivity of human kinin G-protein-
565 coupled receptors. *Nature Chemical Biology*. **14**, 284 (2018).
- 566 25. Pinto, C. et al. Formation of the beta-barrel assembly machinery complex in lipid bilayers
567 as seen by solid-state NMR. *Nature Communications*. **9** (2018).
- 568 26. Good, D. B. et al. Conformational dynamics of a seven transmembrane helical protein
569 Anabaena Sensory Rhodopsin probed by solid-state NMR. *Journal of the American Chemical*
570 *Society*. **136** (7), 2833–2842 (2014).
- 571 27. Medeiros-Silva, J. et al. (1) H-detected solid-state NMR studies of water-inaccessible
572 proteins in vitro and in situ. *Angewandte Chemie (International Edition in English)*. **55** (43),

573 13606–13610 (2016).

574 28. Jekhmene, S. et al. Shifts in the selectivity filter dynamics cause modal gating in K(+) channels. *Nature Communications*. **10** (1), 123 (2019).

575

576 29. Schubeis, T., Le Marchand, T., Andreas, L. B., Pintacuda, G. 1H magic-angle spinning NMR evolves as a powerful new tool for membrane proteins. *Journal of Magnetic Resonance*. **287**, 140–152 (2018).

577

578

579 30. Sinnige, T. et al. Solid-state NMR studies of full-length BamA in lipid bilayers suggest limited overall POTRA mobility. *Journal of Molecular Biology*. **426** (9), 2009–2021 (2014).

580

581 31. Sinnige, T. et al. Insight into the conformational stability of membrane-embedded BamA using a combined solution and solid-state NMR approach. *Journal of Biomolecular NMR*. **61** (3–4), 321–332 (2015).

582

583

584 32. Sinnige, T. et al. Conformational plasticity of the POTRA 5 domain in the outer membrane protein assembly factor BamA. *Structure*. **23** (7), 1317–1324 (2015).

585

586 33. Renault, M., Bos, M. P., Tommassen, J., Baldus, M. Solid-state NMR on a large multidomain integral membrane protein: the outer membrane protein assembly factor BamA. *Journal of the American Chemical Society*. **133** (12), 4175–4177 (2011).

587

588

589 34. Doyle, D. A. et al. The structure of the potassium channel: molecular basis of K⁺ conduction and selectivity. *Science*. **280** (5360), 69–77 (1998).

590

591 35. Wylie, B. J., Bhate, M. P., McDermott, A. E. Transmembrane allosteric coupling of the gates in a potassium channel. *Proceedings of the National Academy of Sciences of the United States of America*. **111** (1), 185–190 (2014).

592

593

594 36. Xu, Y., Zhang, D., Rogawski, R., Nimigean, C. M., McDermott, A. E. Identifying coupled clusters of allostery participants through chemical shift perturbations. *Proceedings of the National Academy of Sciences of the United States of America*. **116** (6), 2078–2085 (2019).

595

596

597 37. van der Cruysen, E. A. W., Prokofyev, A. V., Pongs, O., Baldus, M. Probing conformational changes during the gating cycle of a potassium channel in lipid bilayers. *Biophysical Journal*. **112** (1), 99–108 (2017).

598

599

600 38. Varga, K., Tian, L., McDermott, A. E. Solid-state NMR study and assignments of the KcsA potassium ion channel of *S. lividans*. *Biochimica et Biophysica Acta (BBA) - Proteins and Proteomics*. **1774** (12), 1604–1613 (2007).

601

602

603 39. Zhang, D., Howarth, G. S., Parkin, L. A., McDermott, A. E. NMR studies of lipid regulation of the K⁺ channel KcsA. *Biochimica et Biophysica Acta (BBA) - Biomembranes*. 183491 (2020).

604

605 40. Schneider, R. et al. Solid-state NMR spectroscopy applied to a chimeric potassium channel in lipid bilayers. *Journal of the American Chemical Society*. **130** (23), 7427–7435 (2008).

606

607 41. Raleigh, D. P., Levitt, M. H., Griffin, R. G. Rotational resonance in solid-state Nmr. *Chemical Physics Letters*. **146** (1–2), 71–76 (1988).

608

609 42. Schaefer, J., Stejskal, E. O. C-13 nuclear magnetic-resonance of polymers spinning at magic angle. *Journal of the American Chemical Society*. **98** (4), 1031–1032 (1976).

610

611 43. Fung, B. M., Khitrin, A. K., Ermolaev, K. An improved broadband decoupling sequence for liquid crystals and solids. *Journal of Magnetic Resonance*. **142** (1), 97–101 (2000).

612

613 44. Weingarth, M., Bodenhausen, G., Tekely, P. Low-power decoupling at high spinning frequencies in high static fields. *Journal of Magnetic Resonance*. **199** (2), 238–241 (2009).

614

615 45. Loquet, A., Tolchard, J., Berbon, M., Martinez, D., Habenstein, B. Atomic scale structural studies of macromolecular assemblies by solid-state nuclear magnetic resonance spectroscopy.

616

Journal of Visualized Experiments: JoVE. (127) (2017).

46. Zhou, D. H., Rienstra, C. M. High-performance solvent suppression for proton detected solid-state NMR. *Journal of Magnetic Resonance.* **192** (1), 167–172 (2008).

47. Baldus, M., Petkova, A. T., Herzfeld, J., Griffin, R. G. Cross polarization in the tilted frame: assignment and spectral simplification in heteronuclear spin systems. *Molecular Physics.* **95** (6), 1197–1207 (1998).

48. Verel, R., Baldus, M., Ernst, M., Meier, B. H. A homonuclear spin-pair filter for solid-state NMR based on adiabatic-passage techniques. *Chemical Physics Letters.* **287** (3–4), 421–428 (1998).

49. Lewandowski, J. R., Sass, H. J., Grzesiek, S., Blackledge, M., Emsley, L. Site-specific measurement of slow motions in proteins. *Journal of the American Chemical Society.* **133** (42), 16762–16765 (2011).

50. Sauvee, C. et al. Highly efficient, water-soluble polarizing agents for dynamic nuclear polarization at high frequency. *Angewandte Chemie (International Edition in English).* **52** (41), 10858–10861 (2013).

51. Zhai, W. et al. Postmodification via thiol-click chemistry yields hydrophilic trityl-nitroxide biradicals for biomolecular high-field dynamic nuclear polarization. *The Journal of Physical Chemistry. B.* **124** (41), 9047–9060 (2020).

52. Ghosh, R., Kragelj, J., Xiao, Y., Frederick, K. K. Cryogenic sample loading into a magic angle spinning nuclear magnetic resonance spectrometer that preserves cellular viability. *Journal of Visualized Experiments: JoVE.* (163) (2020).

53. Narasimhan, S. et al. Characterizing proteins in a native bacterial environment using solid-state NMR spectroscopy. *Nature Protocols.* In Press (2020).

54. Ni, Q. Z. et al. High frequency dynamic nuclear polarization. *Accounts of Chemical Research.* **46** (9), 1933–1941 (2013).

55. Weingarth, M. et al. Quantitative analysis of the water occupancy around the selectivity filter of a K⁺ channel in different gating modes. *Journal of the American Chemical Society.* **136** (5), 2000–2007 (2014).

56. Lalli, D. et al. Proton-based structural analysis of a heptahelical transmembrane protein in lipid bilayers. *Journal of the American Chemical Society.* **139** (37), 13006–13012 (2017).

57. Schubeis, T. et al. A beta-barrel for oil transport through lipid membranes: Dynamic NMR structures of AlkL. *Proceedings of the National Academy of Sciences of the United States of America.* **117** (35), 21014–21021 (2020).

58. Baker, L. A., Daniels, M., van der Cruysen, E. A. W., Folkers, G. E., Baldus, M. Efficient cellular solid-state NMR of membrane proteins by targeted protein labeling. *Journal of Biomolecular NMR.* **62** (2), 199–208 (2015).

59. Linser, R. et al. Proton-detected solid-state NMR spectroscopy of fibrillar and membrane proteins. *Angewandte Chemie (International Edition in English).* **50** (19), 4508–4512 (2011).

60. Shukla, R. et al. Mode of action of teixobactins in cellular membranes. *Nature Communications.* **11** (1), 2848 (2020).

61. Kaplan, M. et al. Probing a cell-embedded megadalton protein complex by DNP-supported solid-state NMR. *Nature Methods.* **12** (7), 649–652 (2015).

62. Visscher, K. M. et al. Supramolecular organization and functional implications of K⁽⁺⁾ channel clusters in membranes. *Angewandte Chemie (International Edition in English).* **56** (43),

- 661 13222–13227 (2017).
- 662 63. Narasimhan, S. et al. DNP-supported solid-state NMR spectroscopy of proteins inside
663 mammalian cells. *Angewandte Chemie (International Edition in English)*. **58** (37), 12969–12973
664 (2019).
- 665 64. Wu, R., Stephenson, R., Gichaba, A., Noinaj, N. The big BAM theory: An open and closed
666 case? *Biochimica et Biophysica Acta (BBA) - Biomembranes*. **1862** (1), 183062 (2020).
667

Figure1

[Click here to access/download;Figure;Figure1.pdf](#)

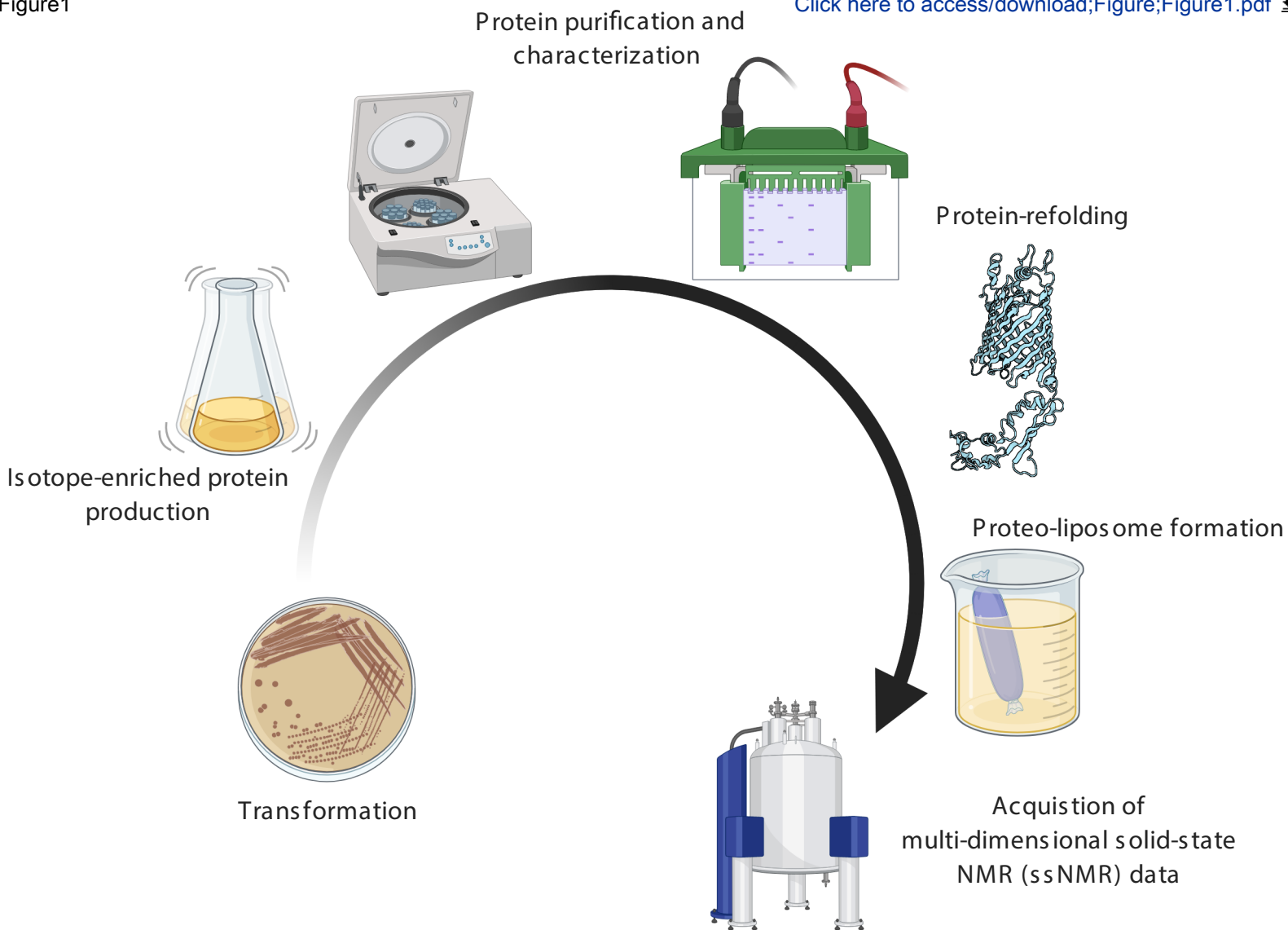


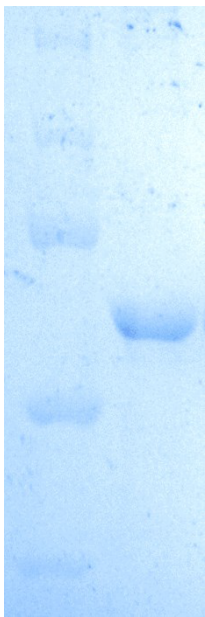
Figure 2

A

A

B

150
100
75
50
37

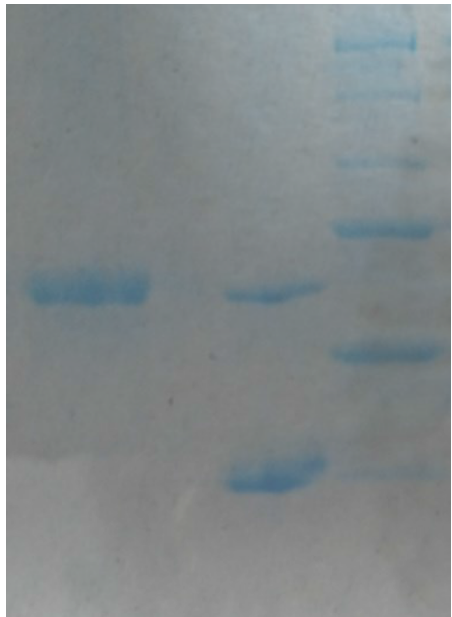


B

A

B

150
100
75
50
37



[Click here to access/download/](#)Figure;Figure



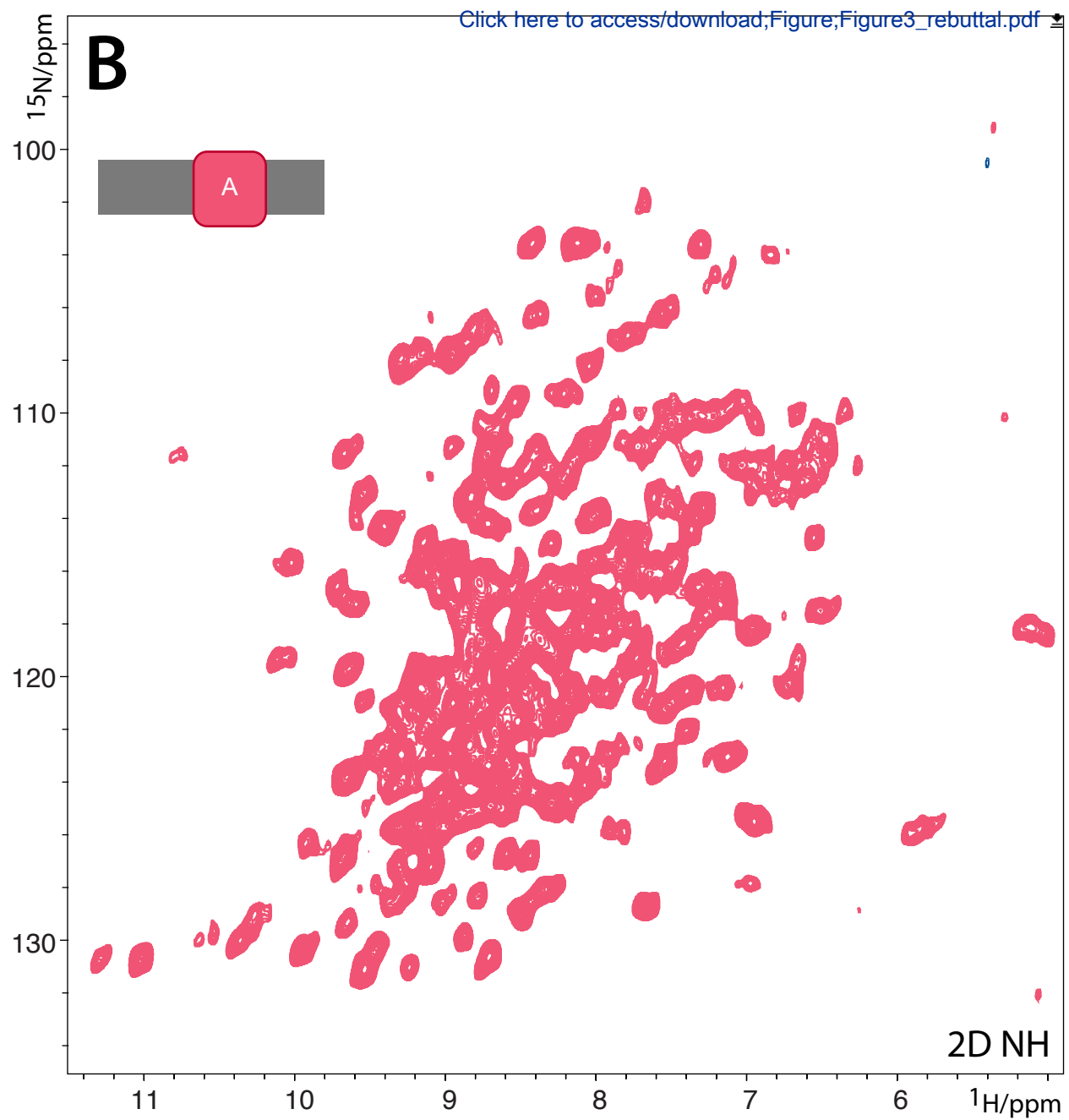
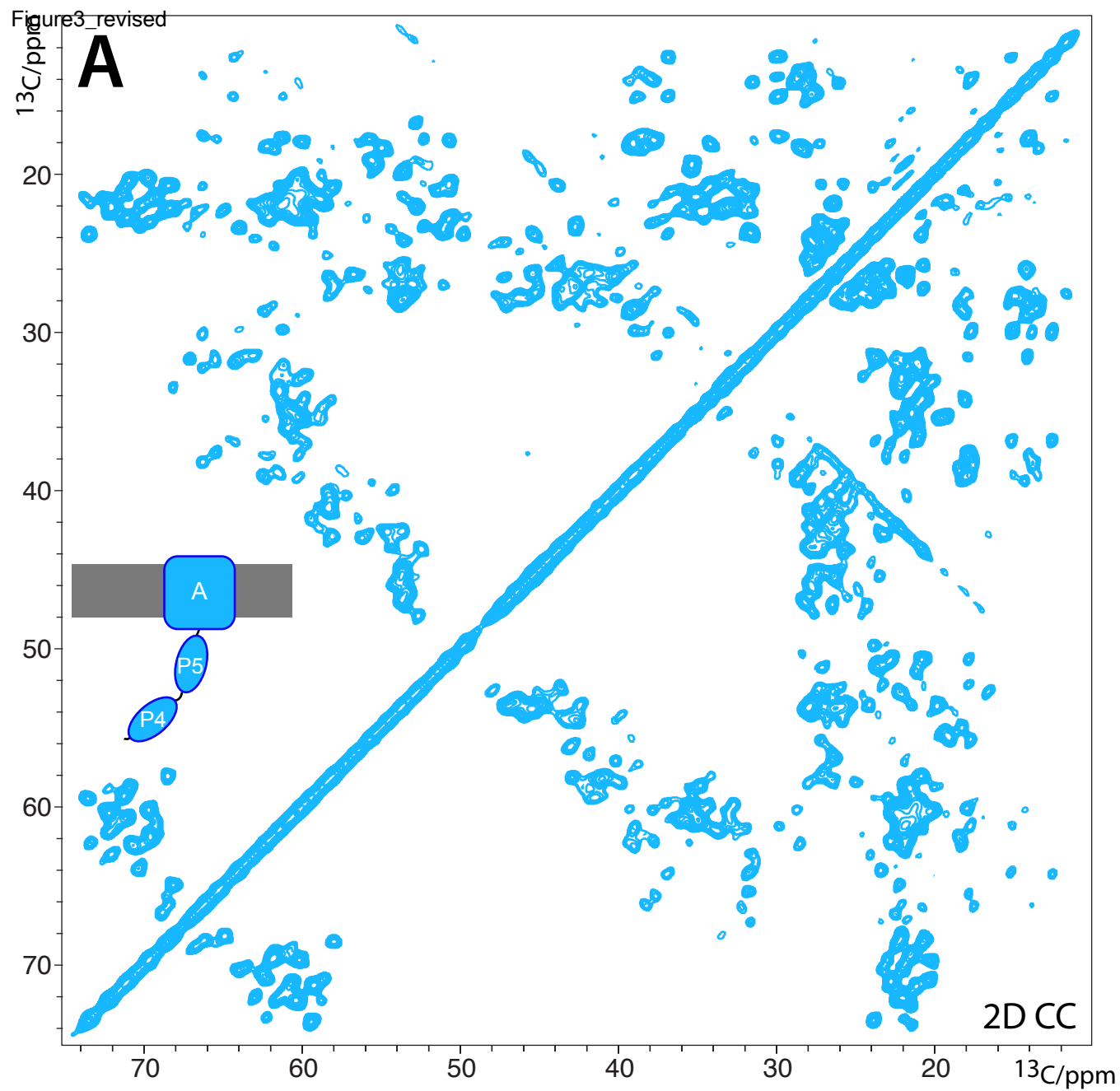
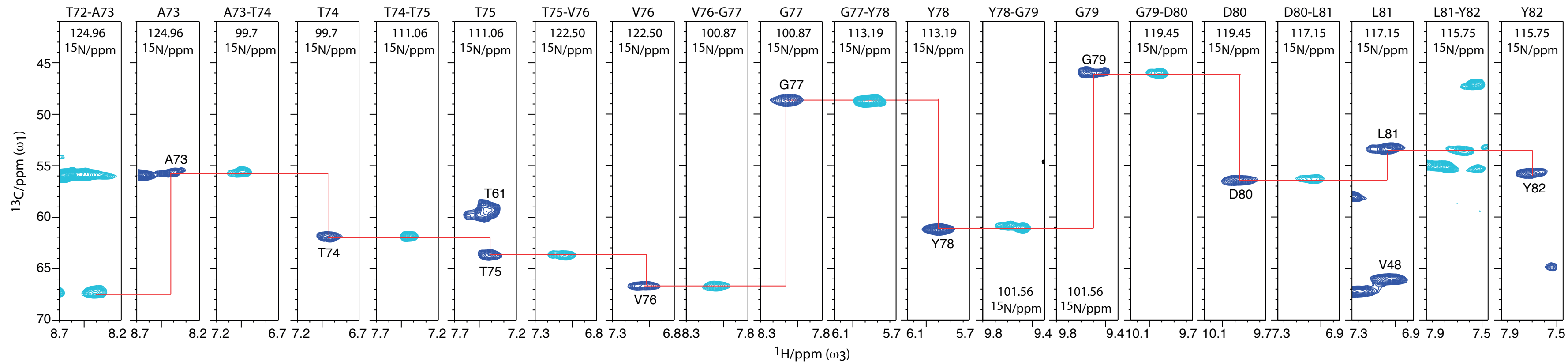
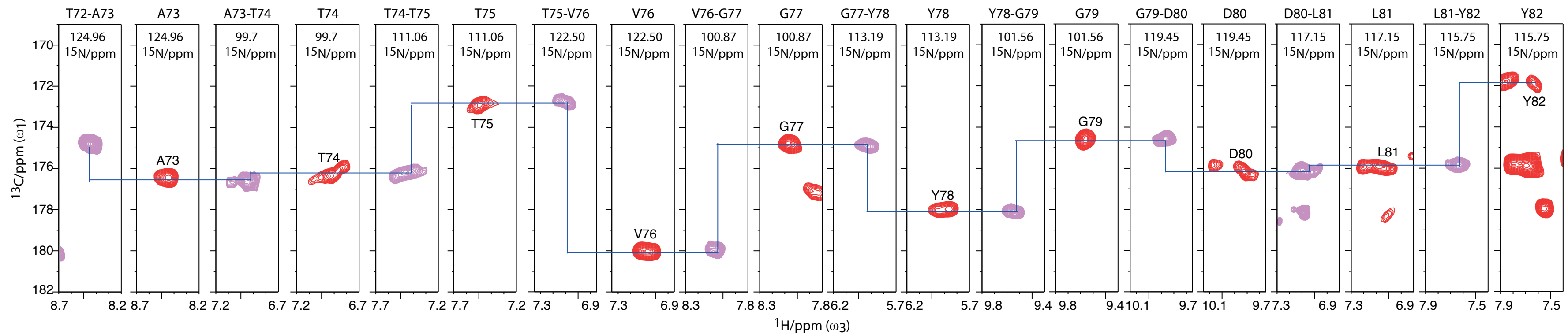


Figure4

C α backbone walk

[Click here to access/download;Figure;Figure4.pdf](#)

CO backbone walk



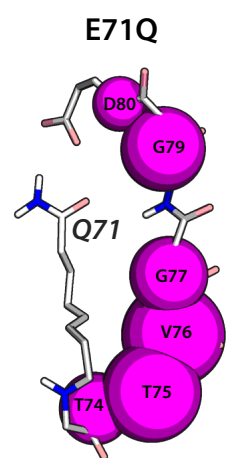
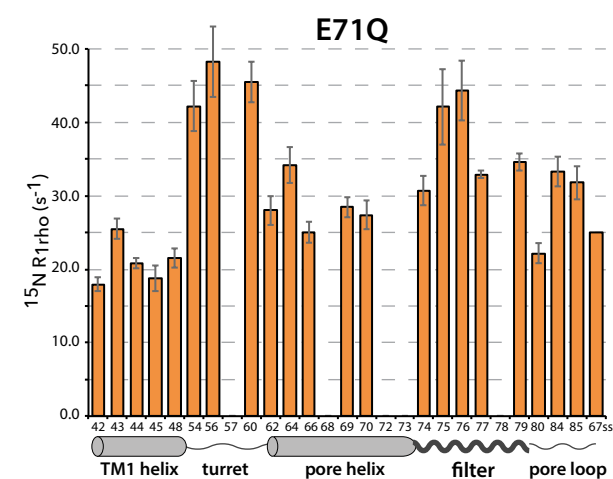
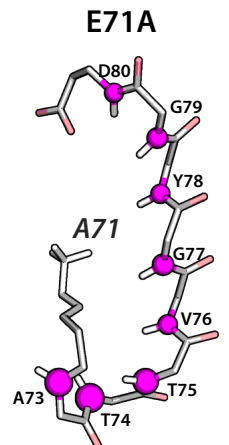
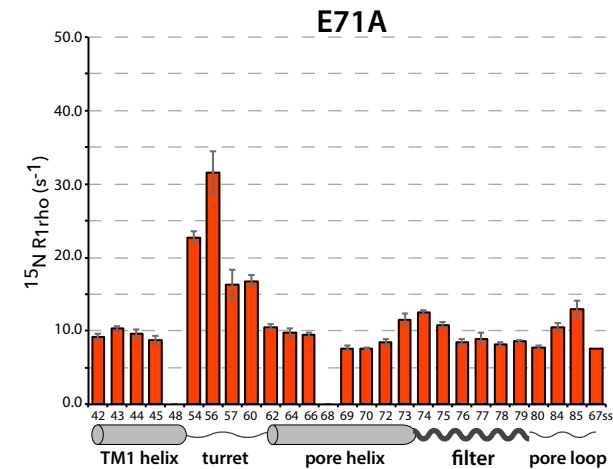
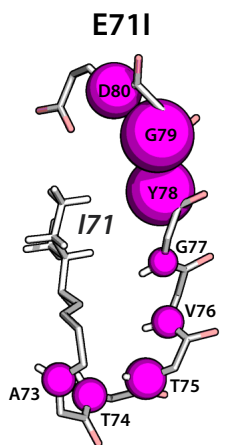
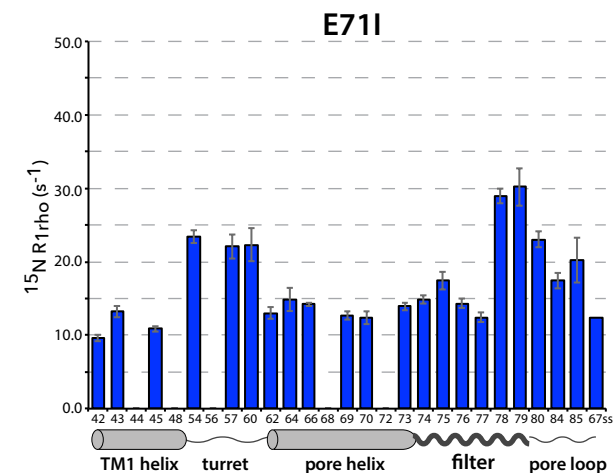
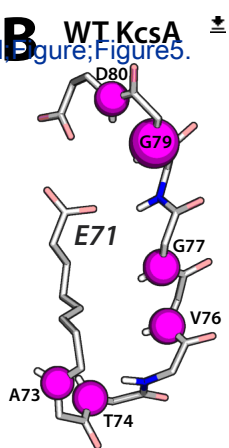
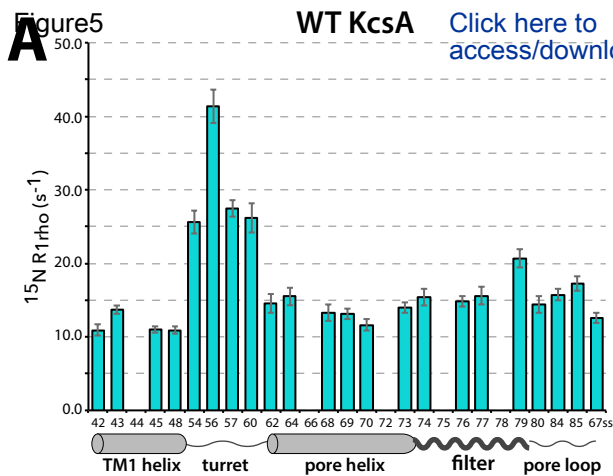


Figure6

[Click here to access/download;Figure;Figure6.pdf](#) 

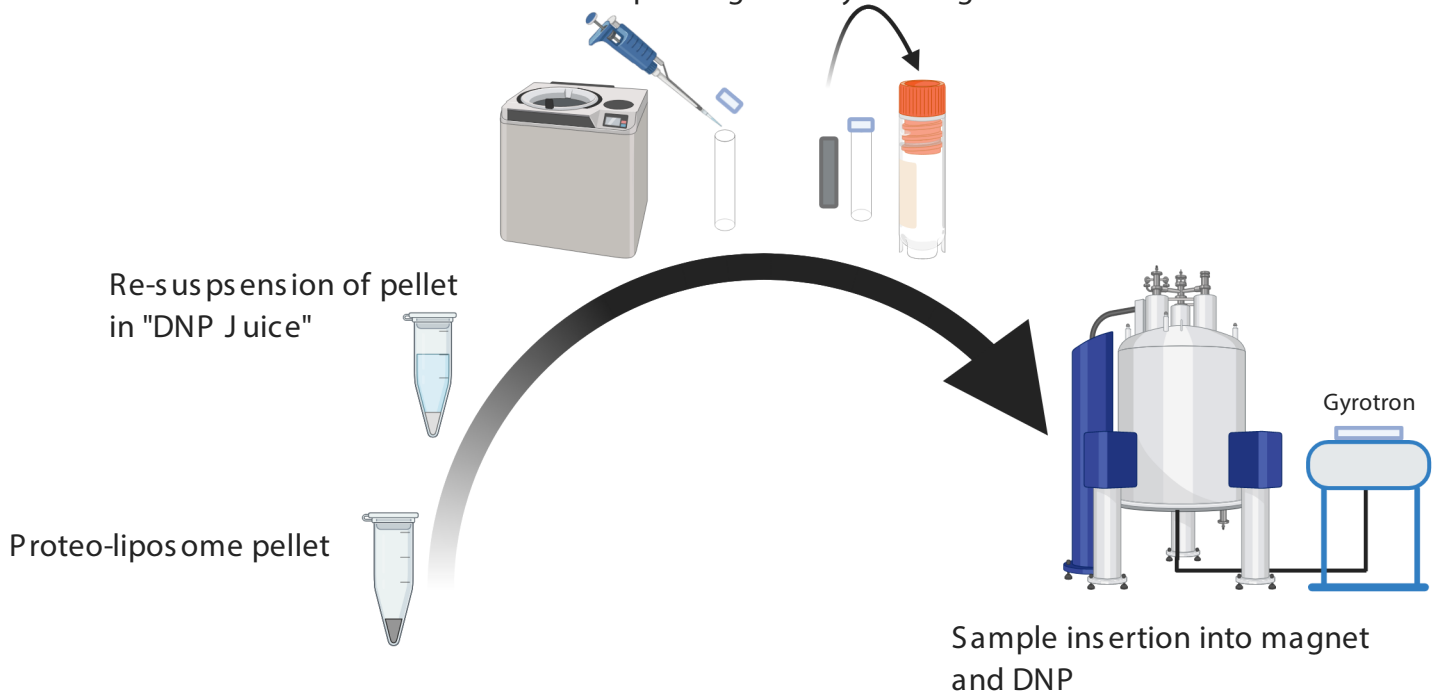


Figure7

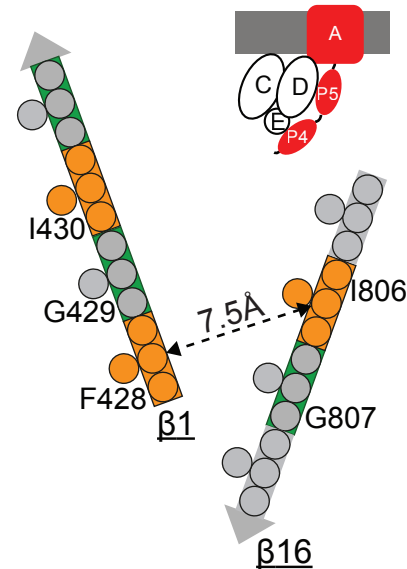
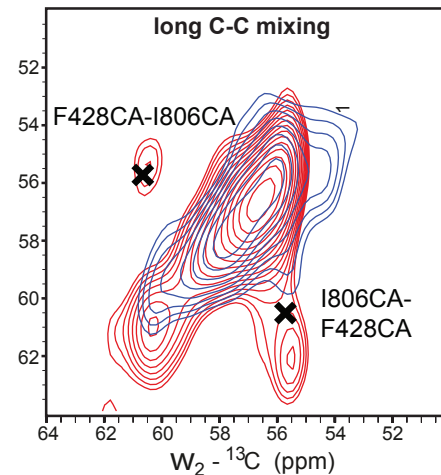
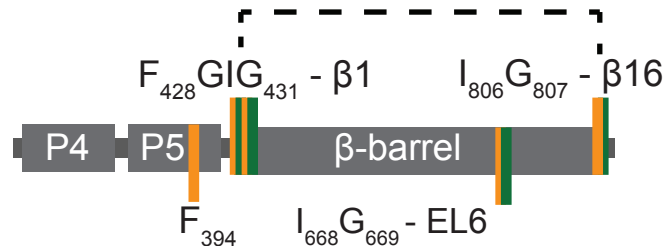
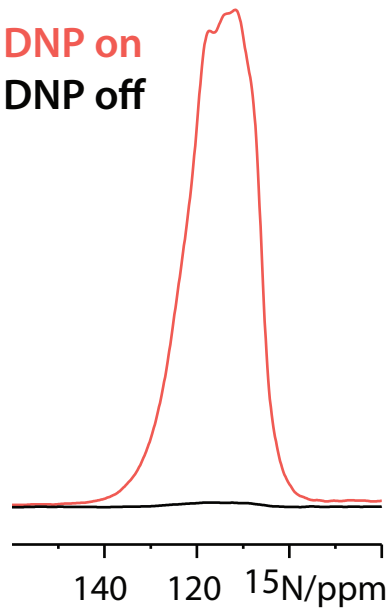
[Click here to access/download:Figure:Figure7.pdf](#)**LATERAL GATE OPEN****DNP on**
DNP off

Table 1. M9 minimal medium recipe

Chemical
Disodium phosphate
Monopotassium phosphate
Sodium Chloride
Ammonium Chloride – both nitrogen-15 enriched and not enriched
Magnesium sulphate (1 M)
Calcium dichloride (1 M)
Iron sulphate (0.01 M)
Isotope enriched glucose*
Glucose
Thiamine (0.5 mg/mL)
Micronutrients
Vitamin Supplements
Ampicillin (50 mg/mL)

Amount/Volume for 1L of Medium

6.0 g

3.0 g

0.5 g

0.5 g

2 mL

10 µL

1 mL

2 g

5 g

10 mL

1 mL

1 mL

1 mL

Chemical	Final Concentration
Buffer 1	
Tris-HCl pH 8.0	50 mM
EDTA	40 mM
Buffer 2	
Tris-HCl pH 8.0	50 mM
EDTA	40 mM
Lysozyme	.2 mg/mL
Sucrose	25%
Buffer 3	
Tris-HCl pH 8.0	10 mM
Buffer 4	
Tris-HCl pH 8.0	10 mM
MgCl ₂	2 mM
Benzonase (>90%)	40 units
Sucrose	25%
DDM	0.10%
Protease inhibitor cocktail in DMSO	1x
Buffer 5	
Tris-HCl pH 8.0	100 mM
Glycine	500 mM
Buffer 6	
Sodium Phosphate pH 7	50 mM
lauryl-dimethylamine oxide (LDAO)	1%
Protease inhibitor cocktail in DMSO	1x

Buffer 7	
Sodium Phosphate pH 7	20 mM
MgCl ₂	5 mM
Buffer 8	
Tris-HCl pH 6.8	62.5 mM
Sodium dodecyl sulfate	0.10%
Glycerol	10%
Bromophenol blue	0.00%

Table 3. Micronutrients stock (1000x)

Chemical	Concentration (mol/L)
Ammonium molibdate	3×10^{-6}
Boric acid	4×10^{-4}
Cobalt chloride	3×10^{-5}
Copper sulphate	1×10^{-5}
Manganese chloride	8×10^{-5}
Zinc chloride	1×10^{-5}

Note: The stock can be made up in water or varying amounts of D₂O as directed by

the protocol.

Table 4. Vitamin Supplement (1000x) for 100 mL

Chemical	Amount (mg) for 100 mL of Supplement
D-Biotin	100
Choline chloride	50
Folic acid	50
Myoinositol	100
Nicatinamide	50
Panthotenic acid	50
Pyridoxal-HCl	50
Riboflavin	5
Thiamine-HCl	50

Note: The supplement can be made up in H₂O or varying amounts of D₂O as directe

d by the protocol.

Reagents

Compound	Supplier
Ammonium molibdate	Merck
Ammonium-15N Chloride	Cortecnet
Ampicillin	Sigma Aldrich
AMUpol	Cortecnet
Benzonase	EMD Millipore Corp
Boric acid	Merck
bromophenol blue	Sigma
calcium dichloride	Merck
Choline chloride	Sigma
Cobalt chloride	Merck
Copper sulphate	Merck
D-Biotin	Merck
Deuterium Oxide	Cortecnet
Dimethyl sulfoxide	Merck
Ethylenediaminetetraacetic acid	Sigma Aldrich
Folic acid	Sigma
Glucose 13C + 2H	Cortecnet
Glycerol	Honeywell
Glycerol (12C3, 99.95% D8, 98%)	Eurisotope
glycerol (non-enriched)	Honeywell
Glycine	Sigma Aldrich
Guanidine hydrochloride	Roth Carl
Iron sulphate	Merck
isopropyl β -D-1-thiogalactopyranoside	Thermofisher
Lysogeny Broth	Merck
Lysozyme	Sigma Aldrich
Magnesium chloride - hexahydrate	Fluka
magnesium sulphate	Merck
monopotassium phosphate	Merck
Myoinositol	Sigma
n-Dodecyl-B-D-maltoside	Acros Organics
N,N-Dimethyldodecylamine N-oxide	Merck
Nicatinamide	Sigma
Panhotenic acid	Sigma
protease inhibitor	Sigma
Pyridoxal-HCl	Sigma Aldrich
Riboflavin	Aldrich
Sodium Chloride	Merck
Sodium dihydrogen phospahte - monohydrate	Sigma Aldrich
Sodium dodecyl sulfate	Thermo-scientific
Sodium hydroxide	Merck

Sucrose	Sigma Life Science
Thiamine-HCl	Merck
Tris-HCl	Sigma Aldrich
Zinc chloride	Merck

Cell Line

Cell Line	Supplier
E.coli BL21 DE3*	New England Biolabs

Equipment

Equipment	Supplier
1.5 mL Ultra-tubes	Beckman Coulter
30 kDa centrifugal filter	Amicon
3.2 mm sapphire DNP rotor with caps	Cortecnet
3.2 mm teflon insert	Cortecnet
3.2 mm sample packer/unpacker	Cortecnet
3.2 mm Regular Wall MAS Rotor	Cortecnet
3.2 mm Regular Wall MAS rotor	Cortecnet
Tool Kit for 3.2 mm Thin Wall rotor	Cortecnet
1.3 mm MAS rotor + caps	Cortecnet
1.3 mm filling tool	Cortecnet
1.3 mm sample packer	Cortecnet
1.3 mm cap remover	Cortecnet
1.3 mm cap set tool	Cortecnet
Dialysis tubing 12-14 kDa	Spectra/Por
Sharpie - Black	Merck

Catalogue Number
277908
CN80P50
A9518
C010P005
70746-3
B6768
B0126
499609
C-1879
449776
C1297
8512090025
CD5251P1000
D9170
L6876
F-7876
CCD860P50
G7757
CDLM-8660-PK
G7757-1L
50046
NR.0037.1
307718
R0392
L3022
L6876
63064
M5921
1051080050
I-5125
3293702509
40236
N-3376
21210-25G-F
P8849
P9130
R170-6
K51107104914
1,063,461,000
28365
1,064,981,000

S9378
5871
10,708,976,001
208086

Catalogue Number
C2527

Catalogue
357448
UFC903024
H13861
B6628
B6988
HZ16913
HZ09244
B136904
HZ14752
HZ14714
HZ14716
HZ14706
HZ14744
132703
HS15094

Bijvoet Center for Biomolecular Research - Utrecht University

Dr. Markus Weingarth



Utrecht University

DateJanuary 07th, 2021

Phone

+3130 253 9932

Email

m.h.weingarth@uu.nl

Subject: Rebuttal Editorial Comments

Dear Editor,

We would like to thank you very much for carefully reading our manuscript and for your comments and suggestions. We have addressed all editorial comments. With this, we hope that you deem our manuscript suitable for publication.

Yours sincerely



Dr. Markus Weingarth

Associate Professor, NMR Spectroscopy Group
Faculty of Science, Utrecht University
Utrecht, The Netherlands

Dear Editor,

Figures 3, 4, 5, and 7 have been modified from refs. 25 and 28., which are Nature Communications papers. **Nature Communications articles are published [under gold open access license \(CC BY\)](#).**

25 *Pinto, C. et al. Formation of the beta-barrel assembly machinery complex in lipid bilayers as seen by solid-state NMR. Nature Communications. 9, (2018).*

28 *Jekhmane, S. et al. Shifts in the selectivity filter dynamics cause modal gating in K(+) channels. Nat Commun. 10 (1), 123, (2019).*